Molecular theory of smectic ordering in liquid crystals with nanoscale segregation of different molecular fragments

M. V. Gorkunov
Shubnikov Institute of Crystallography, Russian Academy of Sciences, 119333 Moscow, Russia

M. A. Osipov
Department of Mathematics, University of Strathclyde, Glasgow G1 1XH, UK

N. Kapernaum, D. Nonnenmacher, and F. Giesselmann
Institute of Physical Chemistry, University of Stuttgart, DE-70569 Stuttgart, Germany

(Received 7 June 2011; revised manuscript received 21 September 2011; published 21 November 2011)

A molecular statistical theory of the smectic *A* phase is developed taking into account specific interactions between different molecular fragments which enables one to describe different microscopic scenario of the transition into the smectic phase. The effects of nanoscale segregation are described using molecular models with different combinations of attractive and repulsive sites. These models have been used to calculate numerically coefficients in the mean filed potential as functions of molecular model parameters and the period of the smectic structure. The same coefficients are calculated also for a conventional smectic with standard Gay-Berne interaction potential which does not promote the segregation. The free energy is minimized numerically to calculate the order parameters of the smectic *A* phases and to study the nature of the smectic transition in both systems. It has been found that in conventional materials the smectic order can be stabilized only when the orientational order is sufficiently high, In contrast, in materials with nanosegregation the smectic order develops mainly in the form of the orientational-translational wave while the nematic order parameter remains relatively small. Microscopic mechanisms of smectic ordering in both systems are discussed in detail, and the results for smectic order parameters are compared with experimental data for materials of various molecular structure.

DOI: 10.1103/PhysRevE.84.051704 PACS number(s): 64.70.mf, 42.70.Df

I. INTRODUCTION

Smectic liquid crystals are characterised by both orientational and translational ordering of anisotropic molecules with an intimate relationship between different types of order. Smectic soft matter systems are very interesting from the fundamental point of view because of their rich phase diagrams, unique sequences of phase transitions, and a broad variety of different types of ordering which may coexist in the same phase.

In simple smectic phases (i.e., in smectics *A* and *C*) the translational ordering is one dimensional, and the direction of the wave vector of the corresponding density wave is either parallel or tilted with respect to the director which specifies the predominant orientation of primary molecular axes.

The existing molecular theory of smectic phases, starting from the pioneering works of McMillan [1] and Kobayashi [2], is based on a simple interpretation of the smectic ordering, which is mathematically very similar to the one-dimensional crystallization. It is assumed that for a sufficiently high orientational order of elongated molecules the system undergoes a transition from the fluid (nematic) phase into a smectic phase due to attraction and repulsion between molecules as a whole, similarly to the case of molecular crystals. It should be noted, however, that there exists a different microscopic mechanisms of smectic ordering which manifests itself, for example, in lyotropic lamellar phases. In lamellar systems, individual layers are formed as a result of a nanoscale segregation between hydrophilic molecular heads, hydrophobic tails, and water, while the long range periodic structure appears for entropic reasons.

It has also been recognized long ago that an element of nanoscale segregation (e.g., between polarizable cores and alkyl tails of typical mesogenic molecules) may be important even in the case of conventional thermotropic smectic liquid crystals. This idea is supported by recent discovery of a new family of smectic materials of de Vries type that tilt without a significant layer contraction [3–6]. The new materials are composed of molecules which usually possess a fluorinated or a siloxane chain, and thus the tendency for a nanoscale segregation between different molecular fragments is strongly enhanced. Smectic phases in these materials are characterized by abnormally weak orientational order, and as a result there is almost no layer contraction at the smectic *A* to smectic *C* phase transition [7,8]. In these materials the smectic ordering is to a large extent stabilized by the nanoscale segregation, while the orientational ordering is less important than in conventional smectics. Thermotropic ionic liquid crystals [9] may represent another class of materials in which the mechanism of smectic ordering differs significantly from that in conventional smectics. Anisotropic ionic fluids do not exhibit nematic phases, and are not mesogenic at all if the ions are removed. Thus the liquid crystalline properties of these materials are dominated by the smectic ordering which is determined by a segregation of charged molecular fragments. There exist also few flexible mesogens which exhibit thermotropic

smectic phases with very low values of the orientational order parameter [10].

The existing molecular theory of smectic liquid crystals (LCs) is mainly based on the McMillan-Kobayashi approach which has been used by many authors (see, for example, Refs. [11–14]), and this simple theory yields a number of results which are in qualitative agreement with experiment. At the same time, it cannot be used to distinguish between different mechanisms of smectic ordering because it is based on an oversimplified phenomenological interaction potential. It has been noticed by several authors [15–19] that the model potential used in McMillan-Kobayashi theory does not include terms which describe a coupling between the intermolecular vector and long molecular axes. These terms, however, make a particular contribution to the stabilization of the smectic order [15,16]. Another limitation of the theory is related to the treatment of the period of smectic ordering, which is not determined self-consistently but is considered as an additional parameter.

More advanced molecular theories have been developed [15–17] which take into account the additional terms in the interaction potential and enable one to determine the smectic periodicity by minimization of the free energy. However, these theories also employ model interaction potentials which only reflect the overall anisotropy of the interacting molecules and do not describe an interaction between different molecular fragments.

In this paper we develop a molecular-statistical theory of smectic ordering using two different types of intermolecular interaction potentials. The first potential is the popular Gay-Berne (GB) potential which describes a smooth repulsion and attraction between anisotropic ellipsoidal molecules and does not account for any specific interactions. The second interaction potential explicitly takes into account strong repulsion and/or attraction between particular molecular fragments. The theory is then developed by expanding these potentials in orthogonal invariants where the expansion coefficients are calculated numerically as functions of molecular model parameters. Both translational and orientational order parameters of the smectic A phase are calculated numerically for different temperatures by direct minimization of the free energy. The use of the interaction potentials of different types enables one to consider in detail the two different microscopic mechanisms of smectic ordering including the conventional one related to one-dimensional crystallization and that dominated by nanoscale segregation between different fragments. We also present the experimentally determined smectic order parameter profiles for a number of LC materials of different molecular structure and discuss the nanosegregation effects in these materials.

The paper is arranged as follows. In Sec. II we present the general mean-field theory of the smectic A phase in which the effective interaction potential and the final expression for the free energy depend on generally unknown coefficients which are functions of the smectic wave periodicity. These coefficients are then calculated numerically for two different types of the model interaction potential in Sec. III. In Sec. IV we consider the phase transition into the smectic A phase and present the order parameter profiles calculated numerically by direct minimization of the free energy. These results are compared with experimental data in Sec. V. Finally the discussion is presented in Sec. VI.

II. MOLECULAR-FIELD THEORY OF SMECTIC ORDERING

In the so-called generalized van der Waals approximation [20,21], the intermolecular attraction interaction is taken into account in the mean-field approximation, while the repulsion is supposed to be infinitely strong, that is, molecules are assumed to possess hard elongated cores. Such a steric repulsion gives rise to steric cut-off effects and is taken into account in the second virial approximation. The corresponding free energy of a LC composed of uniaxial molecules can then be expressed in the form

$$\begin{aligned} F = {} & \frac{1}{2}\rho^2 \int f(\mathbf{r}_1,\mathbf{a}_1)\, \Omega(|\mathbf{r}_1-\mathbf{r}_2|-\boldsymbol{\xi}_{1,2}) \\ & \times U_{\mathrm{att}}(\mathbf{a}_1,\mathbf{a}_2,\mathbf{r}_1-\mathbf{r}_2)\, f(\mathbf{r}_2,\mathbf{a}_2)\, d\mathbf{r}_1\, d\mathbf{r}_2\, d\mathbf{a}_1\, d\mathbf{a}_2 \\ & + \frac{1}{2}k_B T\rho^2 \int f(\mathbf{r}_1,\mathbf{a}_1)\, [1-\Omega(|\mathbf{r}_1-\mathbf{r}_2|-\boldsymbol{\xi}_{1,2})] \\ & \times f(\mathbf{r}_2,\mathbf{a}_2)\, d\mathbf{r}_1\, d\mathbf{r}_2\, d\mathbf{a}_1\, d\mathbf{a}_2 \\ & + k_B T\rho \int f(\mathbf{r}_1,\mathbf{a}_1) \ln[f(\mathbf{r}_1,\mathbf{a}_1)]\, d\mathbf{r}_1\, d\mathbf{a}_1, \end{aligned} \tag{1}$$

where ρ is the molecular number density, and the one-particle distribution function f depends on the molecule position and orientation of its long axis $\mathbf{a}$. The distribution function f is normalized as

$$\int f(\mathbf{r},\mathbf{a})\, d\mathbf{r}\, d\mathbf{a} = V, \tag{2}$$

where V is the volume of the LC.

In Eq. (1) the first term is the internal energy of the system which is determined by the attraction interaction potential $U_{\mathrm{att}}(\mathbf{a}_1,\mathbf{a}_2,\mathbf{r}_1-\mathbf{r}_2)$ modulated by anisotropic steric repulsion. The second term is the packing entropy which is determined by hard core repulsion. Here the step-function $\Omega(|\mathbf{r}_1-\mathbf{r}_2|-\boldsymbol{\xi}_{1,2})=0$ if the molecular cores penetrate each other and $\Omega(|\mathbf{r}_1-\mathbf{r}_2|-\boldsymbol{\xi}_{1,2})=1$ otherwise.

One notes that the free energy (1) can be expressed in a standard mean-filed form with the effective potential which is the sum of the attraction interaction potential modulated by the anisotropic shape, and the contribution from the steric repulsion. Such a generalized mean-field approximation yields reasonable qualitative results in the description of thermotropic liquid crystals where the material undergoes a transition into the smectic phase with a decreasing temperature, and there is no coexistence of phases with different density. In contrast, in the case of hard body systems dominated by steric repulsion, the second virial approximation is not sufficient to describe smectic phases [22].

In the smectic A phase the one-particle distribution function $f(\mathbf{r},\mathbf{a})$ possesses the one-dimensional periodicity, that is, it is a periodic function, with a period d, of the coordinate z along the wave vector $\mathbf{k}$ of the smectic density wave, and is independent of the transverse coordinates:

$$f(\mathbf{r},\mathbf{a}) = f(z,\mathbf{a}) = f(z+d,\mathbf{a}). \tag{3}$$

Then, the free energy density (1) per unit area A of a smectic layer can be expressed as

$$F/A = \frac{1}{2}\rho^2 \int f(z_1,\mathbf{a}_1)\, f(z_2,\mathbf{a}_2) \times \int U_{\rm eff}\{\mathbf{a}_1,\mathbf{a}_2,[\mathbf{r}_\perp + \mathbf{k}(z_1 - z_2)]\} \times d\mathbf{r}_\perp\, dz_1\, dz_2\, d\mathbf{a}_1\, d\mathbf{a}_2 + k_B T\rho \int f(z_1,\mathbf{a}_1) \ln[f(z_1,\mathbf{a}_1)]\, dz_1\, d\mathbf{a}_1, \quad (4)$$

where we have introduced the following effective potential:

$$U_{\rm eff}(\mathbf{a}_1,\mathbf{a}_2,\mathbf{r}) = U_{\rm att}(\mathbf{a}_1,\mathbf{a}_2,\mathbf{r})\Omega(|\mathbf{r}| - \boldsymbol{\xi}_{1,2}) + \lambda k_B T\, [1 - \Omega(|\mathbf{r}| - \boldsymbol{\xi}_{1,2})]. \quad (5)$$

Minimizing the functional (4) with respect to the distribution function $f(z,\mathbf{a})$, one obtains the self-consistence equation for the distribution function

$$f(z,\mathbf{a}) = \frac{1}{Z} \exp\left[-\frac{U_{\rm MF}(z,\mathbf{a})}{k_B T}\right], \quad (6)$$

where

$$Z = \frac{A}{V} \int \exp\left[-\frac{U_{\rm MF}(z,\mathbf{a})}{k_B T}\right] dz\, d\mathbf{a}, \quad (7)$$

and where the mean-field potential reads

$$U_{\rm MF}(z,\mathbf{a}) = \rho \int\int f(z - z',\mathbf{a}_2) \times \int U_{\rm eff}[\mathbf{a},\mathbf{a}_2,(\mathbf{r}_\perp + \mathbf{k}z')] d\mathbf{r}_\perp\, dz'\, d\mathbf{a}_2. \quad (8)$$

One notes that if the one-particle distribution function is periodic, the mean-field potential (8) is also a periodic function of z with the same period d. Thus one can expand $U_{\rm MF}$ in cosine Fourier series (taking the phase to be zero when $z = 0$) keeping for simplicity only the first z-dependent term:

$$U_{\rm MF}(z,\mathbf{a}) = U^{(0)}_{\rm MF}(\mathbf{a}) + U^{(1)}_{\rm MF}(\mathbf{a}) \cos\frac{2\pi z}{d}, \quad (9)$$

where

$$U^{(0)}_{\rm MF}(\mathbf{a}) = \frac{1}{d}\int_{-d/2}^{d/2} U_{\rm MF}(z,\mathbf{a})\, dz \quad (10)$$

and

$$U^{(1)}_{\rm MF}(\mathbf{a}) = \frac{2}{d}\int_{-d/2}^{d/2} U_{\rm MF}(z,\mathbf{a}) \cos\frac{2\pi z}{d}\, dz. \quad (11)$$

Substituting Eqs. (9)–(11) into Eq. (8) one obtains

$$U^{(0)}_{\rm MF}(\mathbf{a}) = \frac{\rho}{d}\int\int_{-d/2}^{d/2} f(z',\mathbf{a}_2)\, dz' \int U_{\rm eff}(\mathbf{a},\mathbf{a}_2,\mathbf{r}) d\mathbf{r}\, d\mathbf{a}_2, \quad (12)$$

and

$$U^{(1)}_{\rm MF}(\mathbf{a}) = \frac{2\rho}{d}\int\int_{-d/2}^{d/2} f(z',\mathbf{a}_2) \cos\frac{2\pi z'}{d} dz' \times \int U_{\rm eff}(\mathbf{a},\mathbf{a}_2,\mathbf{r}) \cos(\mathbf{q}\cdot\mathbf{r})\, d\mathbf{r}\, d\mathbf{a}_2, \quad (13)$$

where $\mathbf{q} = 2\pi\mathbf{k}/d$

One can readily see that the mean-field potential is determined by the following integrals:

$$I_0(\mathbf{a}_1,\mathbf{a}_2) = \rho \int U_{\rm eff}(\mathbf{a}_1,\mathbf{a}_2,\mathbf{r})\, d\mathbf{r}, \quad (14)$$

$$I_1(\mathbf{a}_1,\mathbf{a}_2,\mathbf{k},q) = 2\rho \int U_{\rm eff}(\mathbf{a}_1,\mathbf{a}_2,\mathbf{r}) \cos(\mathbf{q}\cdot\mathbf{r})\, d\mathbf{r}. \quad (15)$$

Here the function $I_0(\mathbf{a}_1,\mathbf{a}_2)$ depends only on the angle $\gamma_{1,2}$ between the molecular axes $\mathbf{a}_1$ and $\mathbf{a}_2$. Taking into account that $\mathbf{a}$ is statistically equivalent to $-\mathbf{a}$, the function I_0 can be expanded in Legendre polynomials of even rank:

$$I_0(\mathbf{a}_1,\mathbf{a}_2) = I_0(\gamma_{1,2}) = \sum_{n=0}^{\infty} I_0^{(n)}\, P_{2n}(\mathbf{a}_1\cdot\mathbf{a}_2). \quad (16)$$

Truncating the series at $n = 2$ one obtains in the first approximation

$$I_0(\mathbf{a}_1,\mathbf{a}_2) \approx \text{const} + u\left[\tfrac{3}{2}(\mathbf{a}_1\cdot\mathbf{a}_2)^2 - \tfrac{1}{2}\right], \quad (17)$$

where

$$u = \frac{5\rho}{16\pi^2}\int\int\int \left[\frac{3}{2}(\mathbf{a}_1\cdot\mathbf{a}_2)^2 - \frac{1}{2}\right] U_{\rm eff}(\mathbf{a}_1,\mathbf{a}_2,\mathbf{r})\, d\mathbf{r} d\mathbf{a}_1 d\mathbf{a}_2. \quad (18)$$

In contrast to I_0, the function $I_1(\mathbf{a}_1,\mathbf{a}_2,\mathbf{k},q)$ depends also on the wave vector $\mathbf{k}$ and can be expanded as

$$I_1(\mathbf{a}_1,\mathbf{a}_2,\mathbf{k},q) = \sum_{n=0}^{\infty}\sum_{l=0}^{\infty}\sum_{m=0}^{\min(n,l)} C^{(m)}_{ln}(q) \times P^{(m)}_n(\mathbf{a}_1\cdot\mathbf{k})\, P^{(m)}_l(\mathbf{a}_2\cdot\mathbf{k}) \cos(m\phi), \quad (19)$$

where ϕ is the difference of the azimuthal angles of the vectors $\mathbf{a}_1$ and $\mathbf{a}_2$ in the plane perpendicular to $\mathbf{k}$. The equivalence of $\mathbf{a}$ and $-\mathbf{a}$ enables one to exclude the terms with odd n and l from (19). The permutational symmetry $1 \leftrightarrow 2$ yields the relationship $C^{(m)}_{ln} = C^{(m)}_{nl}$.

Truncating the series and keeping the harmonics with $l,n \leqslant 2$, and also implying that the LC in nematic and smectic A phases is microscopically uniaxial (the mean-field potential is independent of ϕ) one obtains the following approximate expression:

$$I_1(\mathbf{a}_1,\mathbf{a}_2,\mathbf{k},q) = w_0(q) + w_1(q)[P_2(\cos\gamma_1) + P_2(\cos\gamma_2)] + w_2(q)\, P_2(\cos\gamma_1)\, P_2(\cos\gamma_2), \quad (20)$$

where the constants are given by the integrals

$$w_0(q) = \frac{\rho}{4\pi}\int_0^\pi d\gamma_1\, \sin\gamma_1 \int_0^\pi d\gamma_2\, \sin\gamma_2 \times \int_0^{2\pi} d\phi \int U_{\rm eff}(\mathbf{a}_1,\mathbf{a}_2,\mathbf{r}) \cos(q\,\mathbf{k}\cdot\mathbf{r})\, d\mathbf{r}, \quad (21)$$

$$w_1(q) = \frac{5\rho}{4\pi}\int_0^\pi d\gamma_1\, \sin\gamma_1\, P_2(\cos\gamma_1) \int_0^\pi d\gamma_2\, \sin\gamma_2 \times \int_0^{2\pi} d\phi \int U_{\rm eff}(\mathbf{a}_1,\mathbf{a}_2,\mathbf{r}) \cos(q\,\mathbf{k}\cdot\mathbf{r})\, d\mathbf{r}, \quad (22)$$

$$w_2(q) = \frac{25\rho}{4\pi}\int_0^\pi d\gamma_1\ \sin\gamma_1\ P_2(\cos\gamma_1)\int_0^\pi d\gamma_2\ \sin\gamma_2 \times P_2(\cos\gamma_2)\int_0^{2\pi} d\phi\int U_{\rm eff}(\mathbf{a}_1,\mathbf{a}_2,\mathbf{r})\cos(q\ \mathbf{k}\cdot\mathbf{r})\,d\mathbf{r}, \tag{23}$$

Note that $u = w_2(0)/2$.

Substituting now Eqs. (16) and (20) into Eqs. (12) and (13), one obtains the following expression for overall the mean-field potential:

$$U_{\rm MF}(z,\gamma,\varphi) = uSP_2(\cos\gamma) + w_0(q)\psi\cos qz + w_1(q) \times [\psi P_2(\cos\gamma)\cos qz + \Sigma\cos qz] + w_2(q)\Sigma P_2(\cos\gamma)\cos qz, \tag{24}$$

where the scalar order parameters of the smectic A phase are given by the equations

$$\psi = \langle\cos qz\rangle, \tag{25}$$

$$S = \langle P_2(\cos\gamma)\rangle, \tag{26}$$

and

$$\Sigma = \langle P_2(\cos\gamma)\cos qz\rangle, \tag{27}$$

and where the averaging is defined as

$$\langle\bullet\rangle = \frac{1}{d}\int\!\!\int_{-d/2}^{d/2} f(z,\mathbf{a})\ \bullet\ dz\,d\mathbf{a}. \tag{28}$$

The order parameters S, ψ, and Σ, which have been introduced by McMillan, describe different types of molecular ordering in the smectic A phase. The order parameter ψ characterizes the positional ordering of molecular centres regardless of the degree of orientational order. In contrast, the parameter Σ characterizes simultaneous positional and orientational ordering of anisotropic molecules. In certain simple cases, the orientational order may be approximately decoupled from the translational one, and the the parameter Σ may be factorized approximately as $\Sigma \approx S\psi$ [14]. Then Σ is expected to be rather small since both S and ψ are noticeably smaller than 1. On the other hand, large values of Σ indicate that there exist significant correlations between positions and orientations of the molecules in the smectic phase. For example, the orientational order may be significantly higher for molecules located in the smectic planes (i.e., in the vicinity of the maxima of the density wave). In this case the order parameter Σ may be large while the average orientational order parameter S is small.

Substituting the expression for the mean-field potential into Eq. (6) for the one-particle distribution function and then into Eq. (4), one obtains the final expression for the free energy of the smectic A phase:

$$F/V = -\tfrac{1}{2}\rho uS^2 + w_0(q)\psi^2 + 2w_1(q)\psi\Sigma + w_2(q)\Sigma^2 - k_BT\rho\ln Z, \tag{29}$$

One notes that in this form of the free energy, the coupling constants $w_0(q), w_1(q)$, and $w_2(q)$ are some functions of the smectic wave vector q, which, in principle, should be found by minimization of the total free energy of the smectic phase together will all order parameters. It can be shown, however, that in the mean-field type approximation, used in this paper, the minimization of the total free energy (29) is equivalent to that of the averaged pair interaction potential

$$U(q) = w_0(q)\psi^2 + 2w_1(q)\psi\Sigma_k + w_2(q)\Sigma_k^2. \tag{30}$$

At the same time, the minimization of the averaged potential (30) with respect to $q = 2\pi/d$ cannot be performed in the general case because the dependence of the coupling constants $w_0(q), w_1(q)$, and $w_2(q)$ on q is not known in any generic form. In fact, the dependence of the coupling constants on the wave vector q can only be derived using a particular model of the intermolecular interaction potential. One notes that in McMillan type theories the smectic wave vector q is treated as a parameter of the theory and the coupling coefficients are assumed to be constants during minimization of the free energy. In this way it is only possible to provide a qualitative description of the transition into the smectic phase and, in particular, it is impossible to distinguish between different microscopic mechanisms of smectic ordering.

In the following section the coefficients $w_0(q)$, $w_1(q)$, and $w_2(q)$ are calculated numerically as functions of q using two different types of the model intermolecular interaction potential. We first employ the popular GB model potential which is very smooth and can be used to describe an averaged intermolecular interaction without distinguishing between particular molecular fragments. The second model is based on a sum of the background GB interaction and specific interaction potentials between different molecular fragments including both local attraction and repulsion.

III. INTERMOLECULAR INTERACTION POTENTIALS

A. Gay-Berne potential

The GB model interaction potential is a generalization of the Lennard-Jones potential to the case of anisotropic molecules [23–25]:

$$U_{\rm GB}(\mathbf{a}_1,\mathbf{a}_2,\mathbf{r}) = 4\,\varepsilon(\mathbf{a}_1,\hat{\mathbf{r}},\mathbf{a}_2)\{[r/r_0 - \sigma(\mathbf{a}_1,\hat{\mathbf{r}},\mathbf{a}_2) + 1]^{-12} - [r/r_0 - \sigma(\mathbf{a}_1,\hat{\mathbf{r}},\mathbf{a}_2) + 1]^{-6}\}, \tag{31}$$

where the orientation-dependent range is expressed as

$$\sigma(\mathbf{a}_1,\hat{\mathbf{r}},\mathbf{a}_2) = \left\{1 - \frac{\chi}{2}\left[\frac{(\hat{\mathbf{r}}\cdot\mathbf{a}_1 + \hat{\mathbf{r}}\cdot\mathbf{a}_2)^2}{1+\chi\ \mathbf{a}_1\cdot\mathbf{a}_2} + \frac{(\hat{\mathbf{r}}\cdot\mathbf{a}_1 - \hat{\mathbf{r}}\cdot\mathbf{a}_2)^2}{1-\chi\ \mathbf{a}_1\cdot\mathbf{a}_2}\right]\right\}^{-1/2} \tag{32}$$

and where the anisotropic interaction strength reads

$$\varepsilon(\mathbf{a}_1,\hat{\mathbf{r}},\mathbf{a}_2) = \varepsilon_0[1-\chi^2(\mathbf{a}_1\cdot\mathbf{a}_2)^2]^{-1/2} \times \left\{1 - \frac{\chi'}{2}\left[\frac{(\hat{\mathbf{r}}\cdot\mathbf{a}_1 + \hat{\mathbf{r}}\cdot\mathbf{a}_2)^2}{1+\chi'\ \mathbf{a}_1\cdot\mathbf{a}_2} + \frac{(\hat{\mathbf{r}}\cdot\mathbf{a}_1 - \hat{\mathbf{r}}\cdot\mathbf{a}_2)^2}{1-\chi'\ \mathbf{a}_1\cdot\mathbf{a}_2}\right]\right\}^2. \tag{33}$$

Here r_0 is the width of the molecule, and the constants $\chi = (\kappa^2-1)/(\kappa^2+1)$ and $\chi' = (\kappa'^{1/2}-1)/(\kappa'^{1/2}+1)$ are determined by the relative elongation of the molecule κ as well as by the ratio κ' of the well depths for side-to-side and end-to-end molecular orientations. The steric cutoff here can

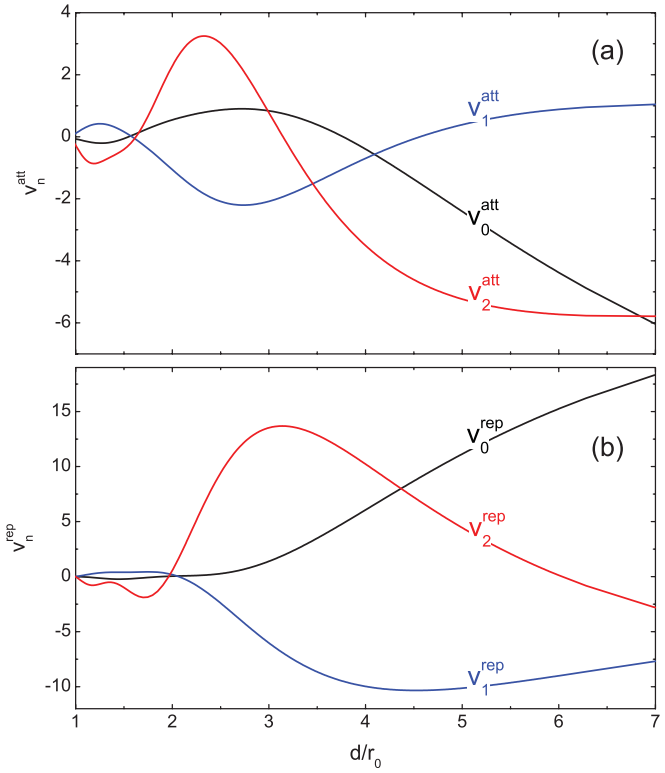

FIG. 1. (Color online) Nondimensional coefficients v_n calculated using the (a) attractive and the (b) repulsive parts of the GB potential with $\kappa = 4$ (molecular elongation) and $\kappa' = 8$ as functions of the smectic layer thickness $d = 2\pi/q$.

be introduced by $\xi_{1,2} = r_0\,\sigma(\mathbf{a}_1,\hat{\mathbf{r}},\mathbf{a}_2)$, and both attraction and steric repulsion are defined self-consistently.

The corresponding coupling constants (21)–(23) (which enter the expression for the free energy) can then be expressed as

$$w_n(q) = 2\rho r_0^3 \varepsilon_0 \left[v_n^{\rm att}(q) + \frac{\lambda k_B T}{\varepsilon_0} v_n^{\rm rep}(q) \right], \qquad (34)$$

where the parameters v are nondimensional and are determined solely by the molecular geometry, that is, by the parameters r_0, κ, and κ'.

The dependence of the coefficients v_n on the smectic layer thickness $d = 2\pi/q$ calculated numerically using the GB potential with representative parameters is shown in Fig. 1.

B. Interactions of molecular centers and tails

In this paper we model the effects of nanoscale segregation by assuming that the elongated molecules possess additional interacting centers including the c centers located at the centers of hard ellipsoids and a symmetric pair of the tail t centers located at the ends of the molecule. The interaction between these groups is mainly determined by the overlapping of localized electron clouds, and we approximate it by the spherical Gaussian potential with characteristic radius equal to a half of molecular breadth, that is, two centers α and β located in different molecules contribute to the

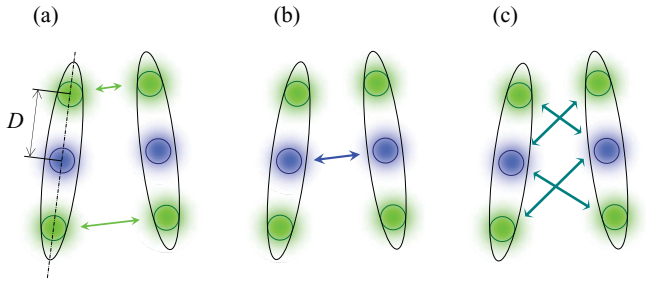

FIG. 2. (Color online) A molecular model which includes interactions between molecular center and tail groups responsible for the nanoscale segregation: (a) attraction of molecular tails, (b) attraction of molecular centers, and (c) repulsion between tails and centers.

potential as

$$U_{\alpha\beta}(r_\alpha\beta) = \varepsilon_{\alpha\beta} \exp\left(-4r_{\alpha\beta}^2/r_0^2\right), \qquad (35)$$

where $r_{\alpha\beta}$ is the distance between the interacting groups and $\varepsilon_{\alpha\beta}$ is the strength of the corresponding interaction.

As illustrated in Fig. 2, generally there are three kinds of specific interactions between different groups: tail-tail (tt), center-center (cc), and center-tail (ct). Then the contributions from the interaction between center and tail fragments are expressed as

$$\begin{aligned} U_{\rm frag}(\mathbf{a}_1,\mathbf{a}_2,\mathbf{r}) = {} & \varepsilon_{\rm cc} \exp\left(-4r^2/r_0^2\right) + \varepsilon_{tt}\left[\exp\left(-4r_{++}^2/r_0^2\right)\right. \\ & + \exp\left(-4r_{--}^2/r_0^2\right) + \exp\left(-4r_{+-}^2/r_0^2\right) \\ & \left. + \exp\left(-4r_{-+}^2/r_0^2\right)\right] + \varepsilon_{ct}\left[\exp\left(-4r_{+c}^2/r_0^2\right)\right. \\ & + \exp\left(-4r_{-c}^2/r_0^2\right) + \exp\left(-4r_{c-}^2/r_0^2\right) \\ & \left. + \exp\left(-4r_{c+}^2/r_0^2\right)\right], \end{aligned} \qquad (36)$$

where the distances are $r_{\pm\pm} = |\mathbf{r} \pm \mathbf{a}_1 D \mp \mathbf{a}_2 D|$, $r_{c\pm} = |\mathbf{r} \mp \mathbf{a}_2 D|$, and $r_{\pm c} = |\mathbf{r} \pm \mathbf{a}_1 D|$.

The nanoscale segregation between molecular fragments is promoted by repulsive tc and attractive tt and cc interactions. Therefore, we assume that the constant $\varepsilon_{\rm ct}$ is positive while the constants $\varepsilon_{\rm tt}$ and $\varepsilon_{\rm cc}$ are negative.

The corresponding contribution to the parameters w_n of the mean-field potential can be written as $2\rho r_0^3 \varepsilon_0 v_n^{\rm f}(q)$, where the dimensionless parameters $v_n^{\rm f}$ can generally be written as sum of three parts:

$$v_n^{\rm f}(q) = \frac{\varepsilon_{\rm cc}}{\varepsilon_0} v_n^{\rm cc}(q) + \frac{\varepsilon_{\rm tt}}{\varepsilon_0} v_n^{\rm tt}(q) + \frac{\varepsilon_{\rm ct}}{\varepsilon_0} v_n^{\rm ct}(q). \qquad (37)$$

Similarly to the previous section, we calculate numerically the integrals in (21)–(23) and obtain the parameters of the mean-field potential. Representative data are given in Fig. 3.

IV. SMECTIC ORDER AND PHASE TRANSITIONS

Introducing the nondimensional temperature

$$\tau = \frac{k_B T}{\varepsilon_0 \rho r_0^3}, \qquad (38)$$

and the nondimensional density

$$\nu = 2\lambda\rho r_0^3, \qquad (39)$$

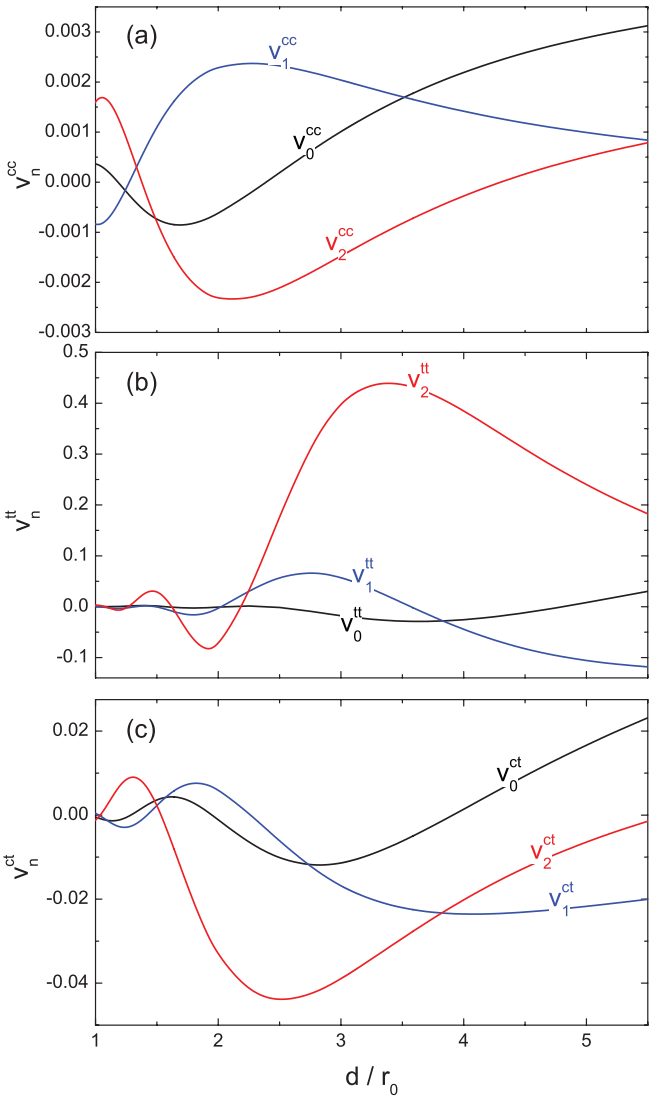

FIG. 3. (Color online) Nondimensional coefficients v_n calculated using (a) center-center and (b) tail-tail attraction interaction as well as (c) tail-center repulsion for $\kappa = 4$ (molecular elongation) and $D = 1.5r_0$ as functions of layer thickness $d = 2\pi/q$.

one can proceed from (29) to the nondimensional free energy defined as $\mathcal{F} = F/(\varepsilon_0\rho^2 V r_0^3)$, which then reads

$$\mathcal{F} = -\tfrac{1}{2}\left(vS^2 + v_0\psi^2 + 2v_1\psi\Sigma + v_2\Sigma^2\right) - \tau \ln Z, \qquad (40)$$

and where

$$Z = \int_{-1}^{1} d\zeta \int d\mathbf{a}\, \exp\left[-\frac{\mathcal{U}(\mathbf{a},\zeta)}{\tau}\right]. \qquad (41)$$

Here the nondimensional mean-field potential

$$\begin{aligned}\mathcal{U}(\mathbf{a},\zeta) = {} & vSP_2(\cos\gamma) + v_0\psi\cos\pi\zeta \\ & + v_1[P_2(\cos\gamma)\psi\cos\pi\zeta\,\Sigma\cos\pi\zeta] \\ & + v_2\Sigma P_2(\cos\gamma)\cos\pi\zeta \end{aligned} \qquad (42)$$

depends on the parameters

$$v_n(d) = v_n^{\rm att}(d) + v\tau v_n^{\rm rep}(d), \quad n = 0,\ 1,\ 2, \qquad (43)$$

while $v = v_2(d \to \infty)/2$. The smectic layer thickness d should be determined by minimization of the following expression:

$$u(d) = v_0(d)\psi^2 + 2v_1(d)\psi\Sigma + v_2(d)\Sigma^2. \qquad (44)$$

A. Smectic ordering of molecules interacting via the Gay-Berne potential

First we minimize numerically the free energy (40) with the parameters v determined by the GB attraction and steric repulsion. It has been found that the intermolecular attraction can stabilize the nematic order, but a substantial contribution from the steric repulsion is also needed to obtain the stable smectic phase and to stabilize the layer thickness in the region slightly larger than the molecular length. In fact, the number density of the molecules has to be closely below the critical value, above which the nematic order may occur due to steric repulsion alone. For molecules with the elongation $\kappa = 4$ this critical density is $\nu_c \approx 0.79$. Minimization of the free energy reveals a distinctive first order transition from the isotropic to the nematic phase and then a second transition into the smectic phase at lower temperature for densities $0.75 < \nu < 0.79$. A typical example of the temperature variation of order parameters in these phases is presented in Fig. 4(a).

At the density $\nu = 0.75$ and lower, the system undergoes a direct transition from the isotropic into the smectic phase.

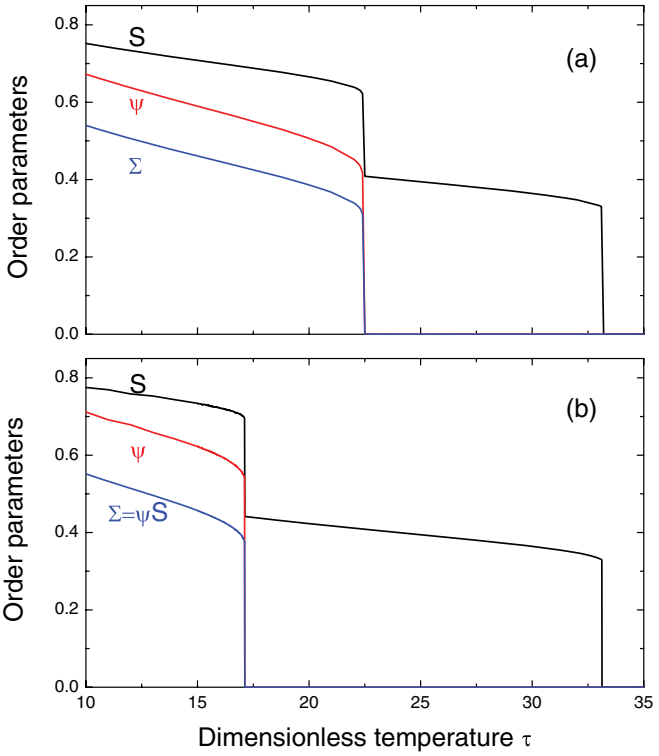

FIG. 4. (Color online) Temperature variation of the order parameters in the isotropic, nematic, and smectic A phases, composed of molecules interacting via the GB potential with $\kappa = 4$, $\kappa' = 8$, and $\nu = 0.77$, calculated by (a) minimization of the original free energy (40), and (b) that with decoupled orientational and translational order (52).

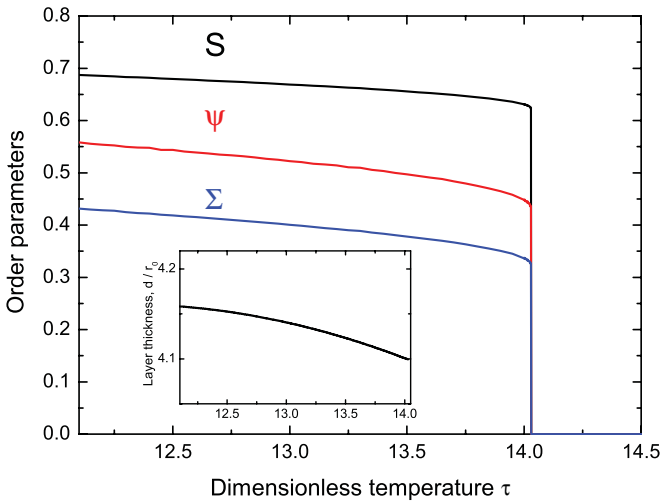

FIG. 5. (Color online) Temperature variation of the order parameters and the smectic layer periodicity (see the inset) at the direct isotropic-smectic A phase transition in the system of molecules interacting via the GB potential with $\kappa = 4$, $\kappa' = 8$, and $\upsilon = 0.75$.

The corresponding order parameter profiles are presented in Fig. 5.

There are two important features characteristic for the order parameters profiles in the system of molecules interacting via the GB potential. First, one notes that all order parameters grow rather slowly with the decreasing temperature both in the nematic and in the smectic A phase. The obvious reason for this is the dominance of steric repulsion in the total intermolecular potential. The smectic layer periodicity, presented in the inset, increases slightly with the decreasing temperature in the smectic A phase, which is in agreement with a typical behavior observed in conventional smectics.

Second, the calculated values of the order parameter Σ appears to be very close (with few percent accuracy) to the product ψS, that is, $\langle P_2(\cos\gamma)\cos qz\rangle \approx \langle P_2(\cos\gamma)\rangle\langle\cos qz\rangle$ at all temperatures, which suggests that the positional and orientational orders are almost statistically independent in this case. This enables one to use a simple approximate model in which the orientational order is decoupled from the positional one.

The decoupling approximation can be made self-consistent by assuming that the original one-particle distribution function is a product of the orientational and the positional distributions:

$$f(\mathbf{r},\mathbf{a}) = f_a(\mathbf{a}) f_z(z). \tag{45}$$

Then the free energy (4) can be minimized separately with respect to both f_a and f_z using the potential (5). Such a procedure yields

$$f_z(z) = \frac{1}{Z_z}\exp\left[-\frac{U_z(z)}{k_B T}\right], \tag{46}$$

$$f_a(\mathbf{a}) = \frac{1}{Z_a}\exp\left[-\frac{U_a(\mathbf{a})}{k_B T}\right], \tag{47}$$

where the separate mean-field potentials are

$$U_z(z) = \psi\cos qz(w_0 + 2w_1 S + w_2 S^2), \tag{48}$$

$$U_a(\mathbf{a}) = uSP_2(\cos\gamma) + \psi^2\{w_0 + w_1[P_2(\cos\gamma) + S] + w_2 S P_2(\cos\gamma)\}, \tag{49}$$

and the partition functions are expressed as

$$Z_z = \frac{A}{V}\int \exp\left[-\frac{U_z(z)}{k_B T}\right] dz, \tag{50}$$

$$Z_a = \int \exp\left[-\frac{U_a(\mathbf{a})}{k_B T}\right] d\mathbf{a}. \tag{51}$$

Substituting the distributions back into the free energy one obtains the following nondimensional free energy of the smectic A phase:

$$\mathcal{F} = -\tfrac{1}{2}[\upsilon S^2 + 3\psi^2(v_0 + 2v_1 S + v_2 S^2)] - \tau \ln Z, \tag{52}$$

where

$$Z = \int_{-1}^{1}\exp\left[-\frac{\mathcal{U}_z(z)}{\tau}\right] dz \int \exp\left[-\frac{\mathcal{U}_a(\mathbf{a})}{\tau}\right] d\mathbf{a}, \tag{53}$$

and where the dimensionless mean-field potentials are expressed as

$$\mathcal{U}_z(z) = \psi\cos\pi z[v_0 + 2v_1 S + v_2 S^2], \tag{54}$$

$$\mathcal{U}_a(\mathbf{a}) = \upsilon S P_2(\cos\gamma) + \psi^2\{v_0 + v_1[P_2(\cos\gamma) + S] + v_2 S P_2(\cos\gamma)\}. \tag{55}$$

Here the parameters v_n are to be evaluated at the thickness d which corresponds to the minimum of the following expression:

$$v_0(d) + 2v_1(d)S + v_2(d)S^2. \tag{56}$$

It is reasonable to expect that the latter is mainly determined by the steric repulsion of molecular cores, that is, by the $v_n^{\mathrm{rep}}(d)$ parts of $w_n(d)$. Corresponding representative curves are shown in Fig. 6. One can readily see that the layer thickness increases with increasing S.

Minimization of the free energy (52) with the interaction constants calculated for the GB potential indeed yields the order parameters close to those obtained by minimizing the more accurate energy (40) as can be seen from comparing Figs. 4(a) and 4(b). As one expects, both approaches also yield

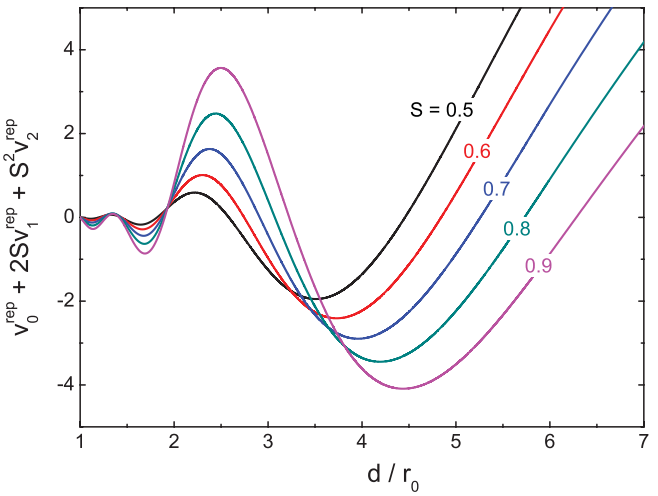

FIG. 6. (Color online) Repulsive contribution to the coupling constants $[v_0^{\mathrm{rep}}(d) + 2v_1^{\mathrm{rep}}(d)S + v_2^{\mathrm{rep}}(d)S^2]$ as a function of the layer spacing d for various values of S calculated for the GB potential with parameters $\kappa = 4$ (molecular elongation) and $\kappa' = 8$.

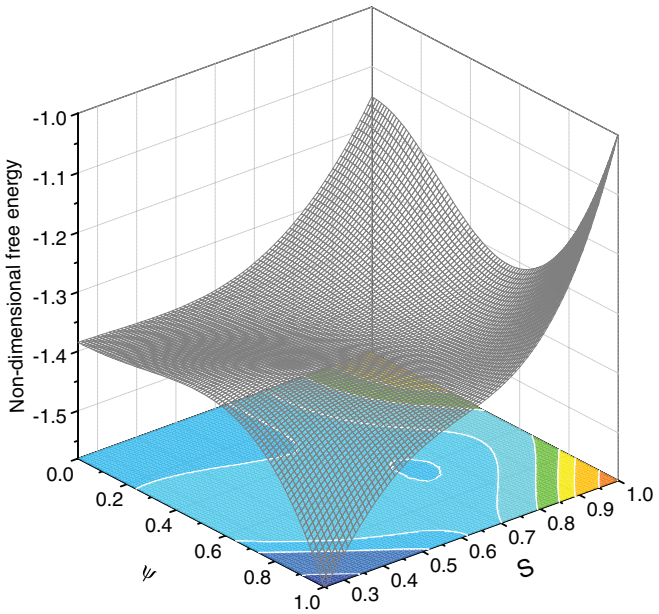

FIG. 7. (Color online) Typical terrain with a shallow minimum at $S \approx 0.734$, $\psi \approx 0.622$, of the nondimensional approximate free energy (52), calculated using the GB interaction potential as a function of the order parameters. The temperature $T = 15$ and concentration $\nu = 0.77$ correspond to the smectic phase below the transition in Fig. 4(b). The layer thickness is taken to be equal to the minimizer of (56) for each combination of the order parameters.

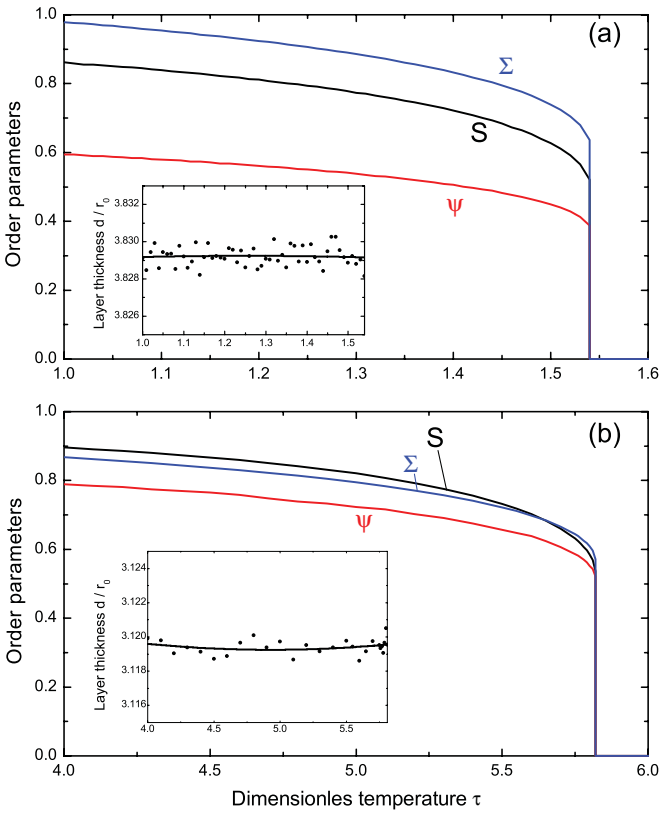

FIG. 8. (Color online) Temperature variation of the order parameters (main) and the smectic layer periodicity (insets: numerical points as dots and polynomial fits as solid lines) at the direct isotropic-smectic A phase transition promoted by the interactions of specific molecular fragments: (a) repulsion between molecular centers and tails $\varepsilon_{ct} = 100\varepsilon_0$, (b) attraction of molecular tails $\varepsilon_{tt} = -100\varepsilon_0$. The tail groups are located at $D = 1.5r_0$, the GB parameters are $\kappa = 4$, $\kappa' = 8$, and the packing entropy is neglected.

the same results in the nematic phase. Although the temperature of the transition into the smectic phase is underestimated in the decoupling approximation, the temperature variation of the order parameters in the smectic A phase is qualitatively the same.

It is interesting to note that both the accurate mean-field free energy and the approximate free energy in the decoupling approximation are generally nonconvex functions of the order parameters. In fact, if one neglects the dependence of the parameters v on the layer thickness, no minima of the free energy can be found. It is due to the variation of v_n with d, which minimizes (30), and, therefore, depends on the order parameters that there appears a shallow minimum of the free energy. A representative complex terrain of the free energy is illustrated in Fig. 7.

B. Smectic phase stabilized by microphase separation

Next we consider the smectic A phase promoted by specific interaction of particular molecular fragments. The latter cannot stabilize the nematic order on their own, and thus we add the attractive part of the GB interaction. However, even in this case the nematic phase cannot be stabilized at temperatures above the smectic A, and as a result the system undergoes only the direct transition from the isotropic to the smectic A phase.

In fact, there are many possibilities to stabilize the smectic A phase combining various terms $\varepsilon_{cc,tt,ct}$ in the interaction potential (36), that is, changing the constants (37). In this paper we consider two different simple cases: positional order induced by mutual attraction of molecular tails, and that induced by the repulsion between molecular centers and tails. One notes that the contribution from the interaction of the localized molecular fragments to the total mean-field potential is much smaller than that from the GB attraction, which is spread over the whole molecular core. Therefore, relatively large values of the interaction constants ε_{ct} and ε_{tt} are required to stabilize the smectic order. We present two typical examples of the isotropic-smectic A phase transition in such a system in Fig. 8.

One can readily see that in this case the relationship between the three order parameters of the smectic A phase is very different compared with the system of molecules interacting via the pure GB potential. In particular, the orientational-translational order parameter Σ is as large as S and may even become the largest order parameter in the smectic phase. In contrast, the purely translational order parameter ψ is smaller than both S and Σ, which obviously means that Σ exceeds substantially the product ψS. As a result, the orientational and translational degrees of freedom cannot be decoupled in this case. Indeed, we were unable to reproduce any of the accurate results using the approximate free energy (52). Thus one concludes that in a system with nanoscale segregation the primary smectic order parameter is the orientational-translational order parameter Σ, and hence the smectic A

phase emerges as an orientational-translational wave, which is different from the one-dimensional crystallization.

It should be noted that in the general case the primary order parameter of a particular phase transition is determined using symmetry arguments, that is, by considering the symmetry groups of the corresponding high and low symmetry phases. For example, the primary order parameter of the smectic A^*-smectic C^* transition is the tilt pseudovector while the polarization and the biaxiality are the secondary order parameters which are induced by the tilt (see, for example, [26]). It is important that in this case the secondary order parameters possess a different symmetry compared to the primary one. In contrast, the two smectic order parameters ψ and Σ possess the same symmetry, and thus the primary smectic order parameter cannot be selected using symmetry arguments alone. At the same time, as discussed above, the parameters ψ and Σ describe different types of smectic ordering, and thus the largest order parameter indicates the primary ordering in a given material.

The temperature variation of the smectic layer periodicity is presented in the insets in Fig. 8. The layer periodicity is approximately constant in this case, that is, the variations are smaller than the accuracy of the performed numerical calculations. A very weak temperature variation of the layer spacing in the smectic A phase is indeed observed in some de Vries type materials with nanoscale segregation (see, for example, [4,7]). At the same time, in some other de Vries type materials the layer spacing slowly increases in the smectic A phase with decreasing temperature [27,28] similarly to conventional smectics. This means that the smectic periodicity may be affected also by other intermolecular interactions which have not been taken into consideration in the present paper. In particular, the effects of molecular biaxiality may be important [29].

The qualitative difference between the smectic order promoted by nanoscale segregation and that, determined by smooth GB intermolecular interaction, can be outlined by considering the spatial distribution of the order parameters across the smectic layer. For this purpose we evaluate the profile of the local density defined as

$$\rho(z) = \int f(\mathbf{a},z)\, d\mathbf{a}, \tag{57}$$

and the profile of the local nematic order parameter

$$S(z) = \frac{\int P_2(\cos\gamma) f(\mathbf{a},z)\, d\mathbf{a}}{\int f(\mathbf{a},z)\, d\mathbf{a}}. \tag{58}$$

Figure 9 shows representative profiles of the number density and the local nematic order parameter below the nematic-smectic A transition in three systems described above: (a) the system of molecules interacting via GB potential, (b) the system with strong repulsion between centers and tails, and (c) the system with strong tail-tail attraction.

One can readily see that the local nematic order profile in the system of molecules interacting via the GB potential is rather similar to the picture assumed in simple molecular theories and, in particular, in phenomenological models. The density of the molecular centers is cosine-like modulated, and their local nematic order is higher in the center of the layers and slightly lower in the region between the layers which is statistically occupied by a smaller fraction of molecules. This explains why the decoupling approximation, which implies the nematic order approximately constant throughout the layer, can be used in this case.

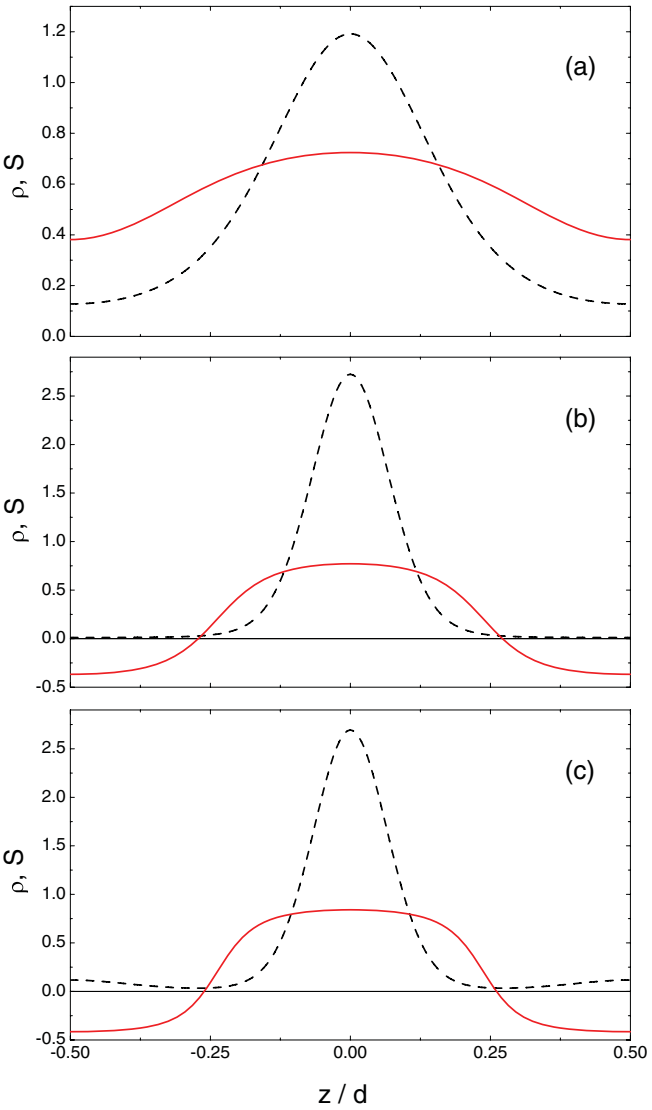

FIG. 9. (Color online) Profiles of the local number density (dashed) and local nematic order parameter (solid) in the smectic A phase: (a) for GB intermolecular interaction as in Fig. 5 at $\tau = 13.5$; (b) for the repulsion between centers and tails as in Fig. 8(a) at $\tau = 1.4$; and (c) for the tail-tail attraction as in Fig. 8(b) at $\tau = 5.5$.

A qualitatively different type of smectic ordering is obtained in the system with nanoscale segregation of molecular fragments. The positional ordering of molecular centers in this case is much closer to the perfect order than to a cosine-like wave. The peaks of the density are much sharper, and a much smaller fraction of molecules can statistically be found between the layers. Moreover, those rare molecules, which occupy the region between the layers, are characterized by a negative local nematic order parameter $S \approx -0.5$, that is, those molecules are aligned in the direction perpendicular to the layer normal.

These different types of smectic ordering on the molecular level can be understood by taking into consideration different relationships between the three order parameters in the smectic A phase discussed above. In a liquid crystal with GB intermolecular interaction potential (see Fig. 5) S and ψ are the largest order parameters, while Σ plays a secondary role being effectively just a product of S and ψ. In contrast, in the smectic phase with nanoscale segregation, the order parameter Σ is the primary order parameter and plays an independent role. One notes that for sufficiently large values of Σ the local nematic order parameter $S(z)$ has to be substantially modulated. In particular, to provide large Σ, the local nematic order $S(z)$ must be negative between the layers in order to sustain the positive values of the product $S(z)\cos qz$ in that region, where the density wave $\cos qz$ is negative.

C. Higher order parameters $\langle P_4(\cos\gamma)\rangle$

The values of the higher order orientational parameters can be very useful for distinguishing the main features of orientational ordering in nematic phase and in the discussed two types of smectic phases. In particular, it is interesting to consider the order parameter $\langle P_4(\cos\gamma)\rangle$ which can be measured experimentally and to compare it with the results obtained using the simple Maier-Saupe orientational distribution function valid for nematic phase. As be shown in the Appendix, using the Maier-Saupe distribution function one can obtain the following simple relationship between the order parameters $S = \langle P_2(\cos\gamma)\rangle$ and $\langle P_4(\cos\gamma)\rangle$:

$$\langle P_4(\cos\gamma)\rangle = \tfrac{1}{12}(7 + 5S - 35\ 0.223\ T/T_N), \qquad (59)$$

where T_N is the isotropic-nematic transition temperature and the orientational distribution function is assumed to be proportional to $\sim\exp[-JSP_2(\cos\gamma)/k_BT]$.

Equation (59) can be used to compare the actual value of the order parameter $\langle P_4(\cos\gamma)\rangle$, calculated in the context of the present theory for different types of intermolecular interaction potential, with the values which correspond to a simple Maier-Saupe orientational distribution in the smectic A phase. The corresponding results are presented in Figs. 10 and 11.

One concludes that none of the molecular models of the smectic A phase under investigation is characterized by a simple Maier-Saupe orientational distribution. However, one can readily see that the actual values of $\langle P_4\rangle$ are closer to the ones obtained from Eq. (59) in the phases composed of molecules interacting via the GB potential. The worst agreement is found in the smectic phase with strong attraction between molecular tails. This deviation is related to the specific profile of $S(z)$ in Fig. 9(c), which is strongly modulated in space.

It is also not surprising that the agreement is not good even for conventional smectics, which can be well described in the decoupling approximation. In this approximation, the mean-field potential (55) contains an extra term $\psi^2 v_1 P_2(\cos\gamma)$,

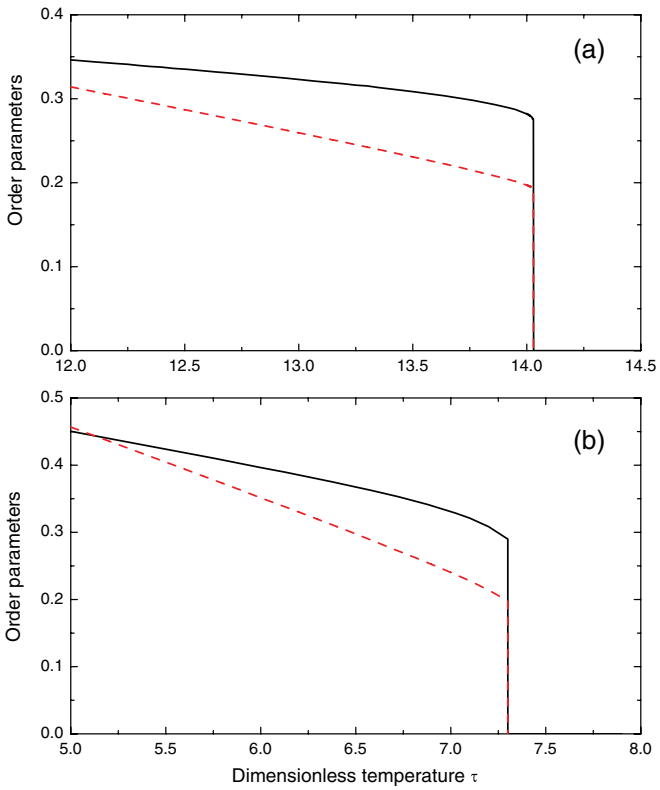

FIG. 10. (Color online) Temperature variation of the calculated order parameter $\langle P_4(\cos\gamma)\rangle$ (solid) and the results for the Mayer-Saupe distribution function (dashed) for liquid crystal with GB intermolecular interactions: (a) with $\nu = 0.75$ as in Fig. 5 and (b) with $\nu = 0.7$.

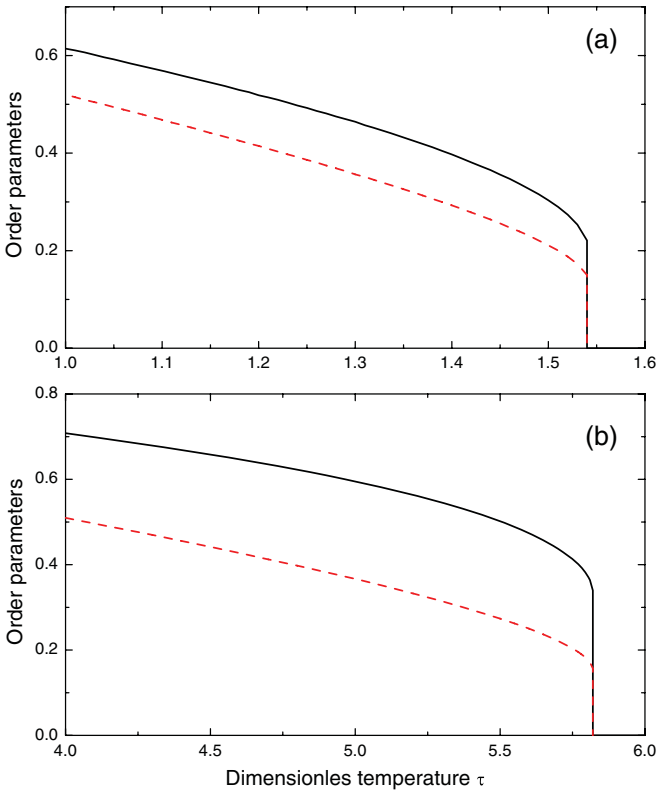

FIG. 11. (Color online) Temperature variation of the order parameter $\langle P_4(\cos\gamma)\rangle$ (solid) and the results for the Maier-Saupe distribution function (dashed) for (a) molecules with the center-tail repulsion as in Fig. 8(a), and (b) molecules with tail-tail attraction as in Fig. 8(b).

which is specific for the smectic phase and which plays the role of the additional ordering field. This term is responsible for the deviation from the results of the Maier-Saupe theory.

V. SMECTIC ORDER PARAMETERS FOR DIFFERENT LIQUID CRYSTAL MATERIALS

One notes that all existing methods which are used to measure the smectic order parameter (see, for example, Refs. [30,31] and references therein) do not enable one to distinguish between parameters ψ and Σ because they possess the same symmetry and thus give similar contributions to major macroscopic quantities. For example, the simple expression for the smectic order parameter proposed by Leadbetter [32] is formally exact only in the limit of very high orientational order when $\psi \approx \Sigma$. In realistic cases the experimental results are rather qualitative, and the measured effective order parameter appears to be a mixture of the purely translational order parameter ψ and the orientational-translational parameter Σ. On the other hand, if the measured smectic order parameter is very large (i.e., of the order of 0.8–0.9), the measurement should be dominated by the order parameter Σ which is the largest parameter in smectic materials with nanoscale segregation between different molecular fragments.

Experimentally determined temperature variation of the smectic order parameter is presented in Fig. 12 for a number of LC materials with different molecular structure which is shown in Fig. 13. The smectic order parameter was determined experimentally by an extrapolation to zero temperature of the temperature-dependent intensity I of the fundamental (001) smectic layer peak, observed in small-angle x-ray scattering experiments. Details of the extrapolation method can be found in Ref. [30]. For the x-ray scattering experiments Ni filtered CuK radiation (wavelength 1.5418 Å) was used. Small angle scattering data from unaligned samples (filled into Mark

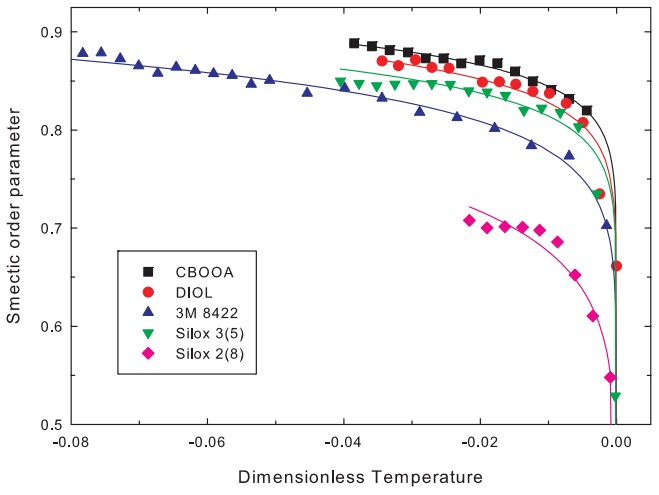

FIG. 12. (Color online) Temperature variation of the smectic order parameter in the smectic A phase for a number of materials with nanoscale segregation including de Vries type LCs with siloxane [Silox 2(8) and Silox 3(5)] and fluorinated (3m) groups, LC with large terminal dipole (CBOOA), and a material with generally nonmesogenic structure and pronounced charge distribution (Diol). See text for a discussion of the molecular structure.

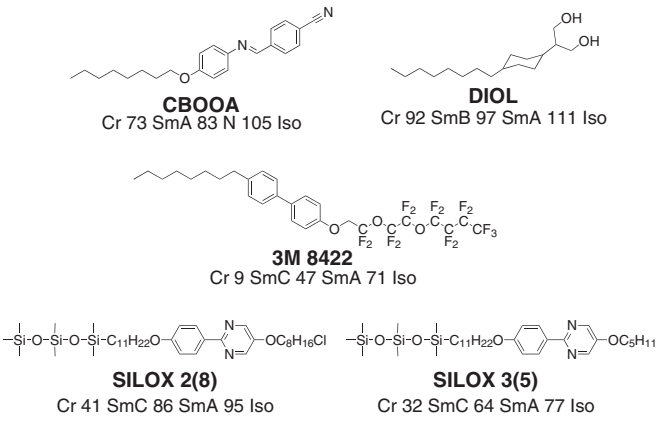

FIG. 13. Schematic molecular structure of the smectic liquid crystal materials CBOOA, Diol, 3M, Silox 2(8), and Silox 3(5) which have been studied experimentally. Temperature variation of the smectic order parameter for these materials is presented in Fig. 12.

capillary tubes of 0.7 mm in diameter) were obtained using a Kratky compact camera (Paar) equipped with a temperature controller (Paar) and a one-dimensional electronic detector (Braun).

One can readily see that completely different LC materials may exhibit very large values of the smectic order parameter. In addition, all these materials are characterized by a specific temperature variation of the smectic ordering. The order parameter grows fast below the transition into the smectic A phase and then rapidly saturates. As shown in this paper, such a temperature variation is typical for smectic materials with strong nanoscale segregation (see Fig. 8). In general, nanoscale segregation is strong when the constituent molecules possess specific groups which strongly repel or attract each other.

In this case there may be a very large energy difference between some mutual configurations of the two molecules. This is apparently the case for the materials Silox 2(8), Silox 3(5), and 3M [30], which possess terminal siloxane or fluorinated groups (see Fig. 13 for the molecular structure). These groups tend to aggregate together promoting the smectic ordering even at low values of the orientational order parameter. These materials are also characterized by de Vries behavior [7,33].

Nanoscale segregation may also be determined by electrostatic interactions between large point molecular dipoles or local charges. For example, the material *CBOOA* is composed of molecules with large longitudinal dipoles determined by the terminal *CN* group (see Fig. 13). In this case, however, the interpretation is not straightforward because a very similar LC material, which differs only by not having the CN group between the two aromatic rings, is characterized by a much lower value of the smectic order parameter [30]. A similar effect can also be observed comparing the two materials Silox 2(8) and Silox 3(5) which both contain the siloxane group and differ mainly by the chlorine atom at the end of the terminal chain (see Fig. 13) [33]. For a yet unknown reason the material with the chlorine is characterized by a much lower value of the smectic order parameter. This indicates that sometimes the nanoscale segregation is a complex phenomenon determined by interactions between multiple molecular fragments which may partially compensate each other.

Another interesting example is the material Diol [10,30] which is composed of molecules that do not possess a typical mesogenic structure (see Fig. 13). The Diol molecules are very flexible and do not exhibit the nematic phase. Even in the smectic *A* phase the orientational order parameter is low [10], and the smectic ordering is apparently stabilized mainly by strong hydrogen bonding between the terminal OH groups and partially by a strong interaction between polar heads which may tend to segregate from the weakly polarizable parts of the molecules. Similar behavior is typical also of ionic liquid crystals [9] which only exhibit smectic phases. Ionic liquid crystals are composed of very flexible molecules which are not mesogenic at all if charges are removed. Smectic ordering can then be stabilized only by strong interaction between local charges and ions.

VI. DISCUSSION

On the molecular level the ordering in the smectic *A* phase is characterized by three order parameters: the orientational order parameter S, the translational order parameter ψ, and the mixed orientational-translational order parameter Σ. One notes that in the existing theories of smectic LCs the role of the order parameter Σ is not emphasized. Indeed, the phenomenological theory is developed in terms of the order parameters S and ψ only [34], while in the molecular theory the parameter Σ is often decoupled as $S\psi$. However, it has been shown in this paper that there exist two different microscopic scenario of the transition into the smectic phase which correspond to different relationships between the mixed order parameter Σ and the parameters S and ψ.

In the model LC composed of molecules interacting via the popular GB potential, the transition into the smectic *A* phase is found to be very close to the "conventional" picture. One notes that the GB potential is very smooth and cannot account for any specific interactions between particular molecular fragments. It has been shown in Sec. III that such a system undergoes a transition into the smectic phase only at sufficiently large value of the nematic order parameter S, that is, the orientational order plays the leading role. In this case the translational order parameter ψ is smaller than S in a broad temperature range below the transition point. At the same time, the mixed order parameter Σ is smaller than both S and ψ and can approximately be decoupled as $\Sigma \approx S\psi$. As shown in Sec. III, the thermodynamical properties of the smectic *A* phase in this case can be described considerably well using this decoupling approximation, that is, it is sufficient to use the parameters S and ψ while the third order parameter Σ plays a secondary role. In this case the transition indeed resembles the one-dimensional crystallization (at least from the mathematical point of view) and is consistent with the "conventional" scenario.

In contrast, in LC materials with strong nanosegregation between different molecular fragments (determined by specific interactions between these fragments), the order parameter Σ plays the leading role at the transition, that is, the smectic phase emerges as an orientational-translational wave. In this case the order parameter Σ is as large as S and can even be large already a few degrees below the transition. At the same time, the purely translational order parameter ψ remains smaller than both Σ and S, which means that Σ cannot be decoupled, and one needs all three order parameters to describe the smectic phase. Relatively low values of S in the smectic *A* phase can be explained qualitatively taking into account that nanoscale segregation promotes the smectic ordering, to some extent, regardless of the degree of orientational order. The system then undergoes the transition into the smectic phase at lower values of S. The transition is governed by the order parameter Σ which rapidly grows directly below the transition point and then saturates at a very high value of about 0.8–0.9. This behavior is observed experimentally for a number of smectic LC materials with nanosegregating groups. At the same time, the parameter ψ is smaller and its behavior is typical of a secondary order parameter which is mainly induced by Σ.

It should be noted that the analysis of different microscopic mechanisms of smectic ordering can only be performed by using particular models for the intermolecular interaction potential and establishing a direct relationship between the parameters of these potentials and the parameters of the statistical theory. In this paper the coefficients of the mean-field free energy of the smectic *A* phase have been calculated numerically for different types of the intermolecular potential as functions of the smectic layer period d. Both the smectic period and all three order parameters have then been calculated numerically as functions of temperature by direct minimization of the free energy.

One notes that the nanoscale segregation model of a smectic LC considered in this paper can be used to explain some properties of de Vries like smectic materials including, in particular, the combination of low orientational and high translational order, and the absence of the nematic phase. On the other hand, the present model is not expected to describe the transition into the smectic *C* phase because it does not take into consideration specific intermolecular interactions [8] which are responsible for the tilt of the director. A detailed description of the smectic *A*-smectic *C* transition in the framework of a more general model may be a subject of a separate study.

ACKNOWLEDGMENTS

This work has been undertaken in the framework of the Materials World Network. M.A.O. is grateful to EPSRC (UK) (Grant EP/H046941/1) for funding, M.A.O. and M.V.G. acknowledge the financial support from the Ministry of Education and Science of Russian Federation (State Contract No. 02.740.11.5169), and F.G., D.N., and N.K. acknowledge the support from DFG (Germany).

APPENDIX: EXPRESSION FOR $\langle P_4(\cos\gamma)\rangle$ WITHIN THE MAIER-SAUPE DISTRIBUTION

Mier-Saupe orientational distribution function of the polar angle γ of long molecular axis reads

$$f(\gamma) = \frac{e^{-JSP_2(\cos\gamma)/k_BT}}{\int_0^\pi d\gamma \sin\gamma\ e^{-JSP_2(\cos\gamma)/k_BT}}. \qquad \text{(A1)}$$

Accordingly, S obeys the equation

$$S = \frac{\int_{-1}^{1} dx\ P_2(x)\, e^{-JSP_2(x)/k_BT}}{\int_{-1}^{1} dx\ e^{-JSP_2(x)/k_BT}}, \tag{A2}$$

which can be reduced to

$$S = \frac{3}{2}\frac{\int_{-1}^{1} dx\ x^2\, e^{-3JSx^2/2k_BT}}{\int_{-1}^{1} dx\ e^{-3JSx^2/2k_BT}} - \frac{1}{2}. \tag{A3}$$

Integrating by parts one obtains

$$S = \frac{k_BT}{2JS} - \frac{1}{2} - \frac{k_BT\ e^{-3JS/2k_BT}}{JS\int_{-1}^{1} dx\ e^{-3JSx^2/2k_BT}}. \tag{A4}$$

On the other hand, the average $\langle \cos^4\gamma \rangle$ reads

$$\langle \cos^4\gamma \rangle = \frac{\int_{-1}^{1} dx\ x^4\, e^{-3JSx^2/2k_BT}}{\int_{-1}^{1} dx\ e^{-3JSx^2/2k_BT}}, \tag{A5}$$

and after integrating by parts this yields

$$\langle \cos^4\gamma \rangle = \frac{2k_BT}{3JS}\left(S + \frac{1}{2}\right) - \frac{2k_BT\ e^{-3JS/2k_BT}}{3JS\int_{-1}^{1} dx\ e^{-3JSx^2/2k_BT}}, \tag{A6}$$

where we have introduced S from Eq. (A3).

Combining Eqs. (A4) with (A6) and excluding the last terms it is easy to get the simple relation

$$\langle \cos^4\gamma \rangle = \frac{2k_BT}{3J} + \frac{2}{3}S + \frac{1}{3}. \tag{A7}$$

Accordingly, the higher order parameter reads

$$\langle P_4(\cos\gamma) \rangle = \frac{35}{12}\frac{k_BT}{J} + \frac{5}{12}S + \frac{7}{12}. \tag{A8}$$

Finally, taking into account that the Maier-Saupe interaction constant J is related to the temperature of the transition from isotropic to orientationally ordered liquid crystal phase $k_BT_N = 0.223J$, one obtains the relation (59).

[1] W. L. McMillan, Phys. Rev. A **4**, 1238 (1971).
[2] K. K. Kobayashi, Mol. Cryst. Liq. Cryst. **13**, 137 (1971).
[3] Y. Takanishi *et al*., Jpn. J. Appl. Phys. Lett. **29**, L984 (1990).
[4] J. Naciri, J. Ruth, G. Crawford, R. Shashidhar, and B. R. Ratna, Chem. Mater. **7**, 1397 (1995).
[5] M. D. Radcliffe, M. L. Brostrom, K. A. Epstein, A. G. Rappaport, B. N. Thomas, and R. F. Shao, and N. A. Clark, Liq. Cryst. **26**, 789 (1999).
[6] F. Giesselmann, P. Zugenmaier, I. Dierking, S. T. Lagerwall, B. Stebler, M. Kaspar, V. Hamplova, and M. Glogarova, Phys. Rev. E **60**, 598 (1999).
[7] J. P. F. Lagerwall and F. Giesselmann, Chem. Phys. Chem. **7**, 20 (2006).
[8] M. V. Gorkunov, M. A. Osipov, J. P. F. Lagerwall, and F. Giesselmann, Phys. Rev. E **76**, 051706 (2007).
[9] K. Binnemans, Chem. Rev. **105**, 4148 (2005).
[10] F. Giesselmann, R. Germer, and A. Saipa, J. Chem. Phys. **123**, 034906 (2005).
[11] F. T. Lee, H. T. Tan, Y. M. Shih, and C.-W. Woo, Phys. Rev. Lett. **18**, 1117 (1973).
[12] P. J. Photinos and A. Saupe, Phys. Rev. A **13**, 1926 (1976).
[13] M. R. Kuzma and D. W. Allender, Phys. Rev. A **25**, 2793 (1982).
[14] G. F. Kventsel, G. R. Luckhurst, and H. B. Zewdie, Mol. Phys. **56**, 589 (1985).
[15] L. Mederos and D. E. Sullivan, Phys. Rev. A **39**, 854 (1989).
[16] B. Tjipto-Margo and D. E. Sullivan, J. Chem.Phys. **88**, 6620 (1978).
[17] J. Stecki and A. Kloczkowski, Mol. Phys. **42**, 51 (1981).
[18] L. Senbetu and C.-W. Woo, Phys. Rev. A **17**, 1529 (1978).
[19] M. D. Lipkin and D. W. Oxtoby, J. Chem. Phys. **79**, 1939 (1983).
[20] M. A. Osipov, in *Handbook of Liquid Crystals*. Vol. 1, 2nd ed., edited by D. Demus, J. Goodby, G. W. Gray, H.-W. Spies, and V. Vill (Wiley-VCH, Weinheim, 1998).
[21] W. M. Gelbart and B. Barboy, Acc. Chem. Res. **13**, 290 (1980).
[22] W. Jozefowicz, G. Cholewiak, and L. Longa, Phys. Rev. E **71**, 032701 (2005).
[23] J. G. Gay and B. J. Berne, J. Chem. Phys. **74**, 3316 (1981).
[24] E. de Miguel, L. F. Rull, M. K. Chalam, K. E. Gubbins, and F. Van Swol, Mol. Phys. **72**, 593 (1991).
[25] R. Berardi, L. Muccoli, S. Orlandi, M. Ricci, and C. Zannoni, J. Phys. Condens. Matter **20**, 463101 (2008).
[26] M. A. Osipov and S. A. Pikin, J. Phys. II **5**, 1223 (1995).
[27] R. Korlacki, V. P. Panov, A. Fukuda, J. K. Vij, C. M. Spillmann, and J. Naciri, Phys. Rev. E **82**, 031702 (2010).
[28] H.-G. Yoon, D. M. Agra-Kooijman, K. Ayub, R. P. Lemieux, and S. Kumar, Phys. Rev. Lett. **106**, 087801 (2011).
[29] M. V. Gorkunov and M. A. Osipov, J. Phys. A **41**, 295001 (2008).
[30] N. Kapernaum and F. Giesselmann, Phys. Rev. E **78**, 062701 (2008).
[31] G. Alexander, S. King, R. Richardson, and H. Zimmermann, Liq. Cryst. **37**, 961 (2010).
[32] A. J. Leadbetter, in *The Molecular Physics of Liquid Crystals*, edited by G. Luckhurst and G. Gray (Academic, London, 1979).
[33] J. Roberts, N. Kapernaum, Q. Song, D. Nonnemacher, K. Ayub, F. Giesselmann, and R. Lemieux, J. Am. Chem. Soc. **132**, 364 (2010).
[34] P. G. de Gennes and J. Prost, *The Physics of Liquid Crystals* (Clarendon, Oxford, 1993).